Molecular Views of Physical Adsorption Inside and Outside of Single-Wall Carbon Nanotubes

PETRO KONDRATYUK AND JOHN T. YATES, JR.*
Surface Science Center, Department of Chemistry, University of Pittsburgh, Pittsburgh, Pennsylvania 15260

Received January 31, 2007

ABSTRACT
We discuss our own studies of molecular adsorption on and inside of single-wall carbon nanotubes in the broader context of important theoretical and experimental developments in the field. We show that adsorption in the nanotube interior sites as well as in the groove and exterior sites may be resolved by various experimental methods. In addition, the changes that the adsorbate phases undergo due to confinement in the nanotube interior are discussed, particularly focusing on confined molecules of water, alkanes, and an alkene. Attention is also devoted to the use of oxidizing agents such as ozone to open the ends and walls of nanotubes for interior adsorption.

1. Introduction

Single-wall carbon nanotubes (SWNTs) occupy an interesting place among carbonaceous adsorptive materials. On one hand, they offer chemically inert surfaces for physical adsorption, and their high specific surface areas are comparable to those of activated carbons (surface areas of up to 1600 m^2/g have been reported[1]). On the other hand, SWNTs are fundamentally different from activated carbons in that their structure at the atomic scale is far more well-defined and uniform. While parameters such as the pore diameter distribution and adsorption energy distribution are needed to quantify adsorption on activated carbons, in the case of carbon nanotubes one can deal directly with various well-defined adsorption sites available to the adsorbing molecules. From the standpoint of structure, the relationship between carbon nanotubes and other carbonaceous adsorptive materials is similar to that between single crystals and polycrystalline materials.

At present, approximately 19,000 papers have been published on carbon nanotubes and approximately 5% of these relate to their adsorption properties. Figure 1 shows the evolution of the total research activity on nanotubes since the discovery of multiwall nanotubes by Iijima in 1991.[2] A doubling of research activity occurs every 2–3 years, even 10 years after the discovery of this interesting allotrope of carbon.

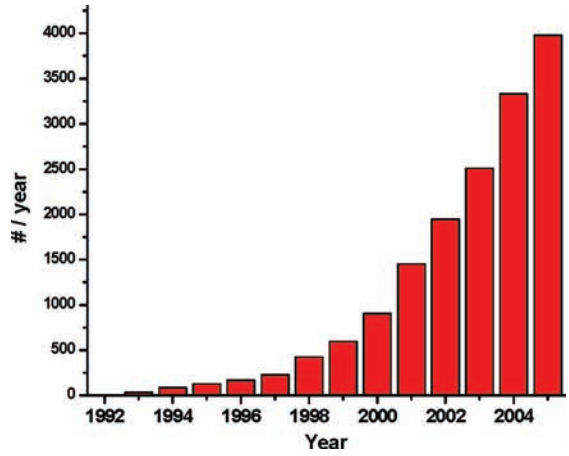

FIGURE 1. Number of scientific publications on carbon nanotubes since their discovery.

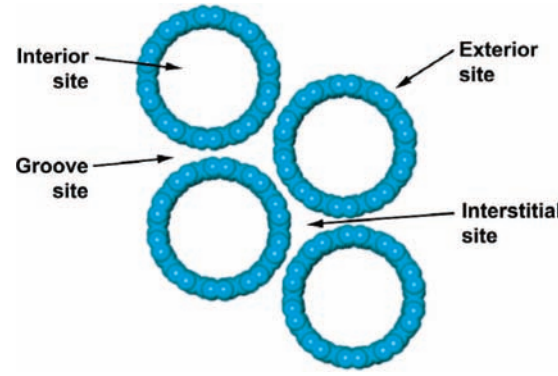

FIGURE 2. Schematic of a hexagonally packed SWNT bundle consisting of four (10,10) nanotubes viewed end-on. Four types of adsorption sites are shown.

Single-wall carbon nanotubes were first experimentally identified by Iijima and Ichihashi[3] and Bethune et al.[4] They consist of sheets of sp^2-hybridized carbon (graphene sheets) rolled into cylinders with diameters ranging from 5–6 to ~20 Å, depending on the particular method and conditions during their synthesis.[5] Lengths typically range in the hundreds of nanometers or micrometers. SWNTs associate with each other due to attractive dispersive forces to form bundles, typically comprising tens or hundreds of individual nanotubes. Adsorption of molecules takes place on these bundles. Thus, to gain insight into adsorption on SWNTs, one needs to consider the structure of the bundle and the adsorption sites available to the adsorbate molecules (Figure 2).

Four types of adsorption sites can be identified: the nanotube interior sites, the sites on the exterior surface, the groove sites, and the interstitial sites. The groove sites

Petro Kondratyuk received his B.S. degree in Chemistry from Kiev National University in Kiev, Ukraine, in 2001. He is currently a graduate student completing his Ph.D. degree under the direction of John T. Yates, Jr., at the Surface Science Center, Department of Chemistry, University of Pittsburgh. The major theme of his research has been the investigation of adsorptive properties of carbon nanotubes using surface science and spectroscopy techniques under ultrahigh vacuum conditions.

Professor Yates is the R. K. Mellon Emeritus Professor of Chemistry at the University of Pittsburgh and has just transferred to The University of Virginia (Charlottesville, VA), where he is Professor and Shannon Fellow in the Department of Chemistry. He received his B.S. degree from Juniata College (Huntingdon, PA) and his Ph.D. from the Massachusetts Institute of Technology (Cambridge, MA). He is a member of the National Academy of Sciences. His research interests in many areas of surface chemistry and physics are reported in more than 600 publications and result from the mentoring of more than 40 Ph.D. students.

* Corresponding author. E-mail: johnt@virginia.edu.

10.1021/ar700013c CCC: $37.00
Published on Web 07/04/2007

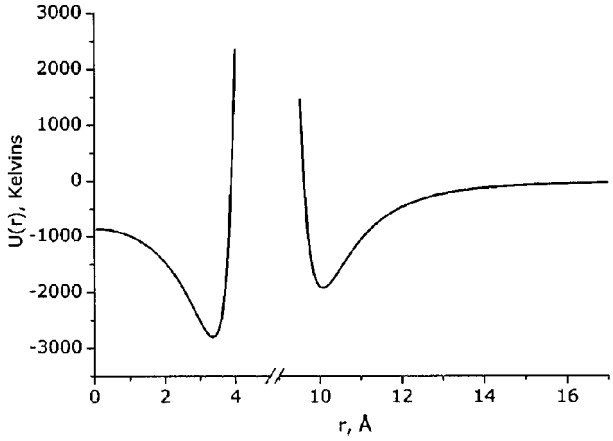

FIGURE 3. Interaction potential for a Xe atom in the vicinity of a (10,10) SWNT. The zero on the distance axis corresponds to the center of the nanotube. The curve on the left corresponds to a Xe atom inside the SWNT, while that on the right corresponds to a Xe atom outside of the SWNT. Reused with permission from Vahan V. Simonyan, Journal of Chemical Physics, 114, 4180 (2001). Copyright 2001, American Institute of Physics.

are narrow troughs formed on the outside of the bundles where a pair of nanotubes meet. The interstitial sites are channels between individual nanotubes inside the bundle. Theoretical results predict that the smallest adsorbate molecules (such as H_2, He, and Ne) can access the interstitial sites and be adsorbed there.[6] However, several experimental studies have failed to observe adsorption in the interstitial sites.[7–9]

The nanotube interior is expected to have a high binding energy toward adsorbing molecules because the closeness of the surrounding walls to the adsorbed molecule maximizes the attractive van der Waals interaction. On the other hand, on the nanotube exterior the walls curve away from the adsorbed molecules, meaning that the adsorption energy must be smaller compared to that for the interior and for flat graphene. This intuitive picture is corroborated by molecular simulations[10,11] and experimental results.[12] Simonyan et al.[11] calculated the potential energy of a Xe atom in the interior and on the exterior of a (10,10) single wall nanotube having a diameter of 13.6 Å. The plot of the potential energy versus distance from the nanotube center is shown in Figure 3. The difference between the adsorption energies for the interior and exterior surfaces was found to be 800 K. An experimental estimate of the binding energy of Xe on untreated (closed) carbon nanotubes was recently provided by Rawat et al.[12] The authors placed this value at 256 meV (2970 K), which is ~60% higher than the binding energy of Xe on a flat graphite surface.

As far as the adsorption energies for the groove sites are concerned, theoretical and experimental work has shown that the adsorption energy for groove sites present on the exterior of the SWNT bundles lies between the adsorption energies for exterior and interior sites.[13] This will be discussed in more detail in section 3.

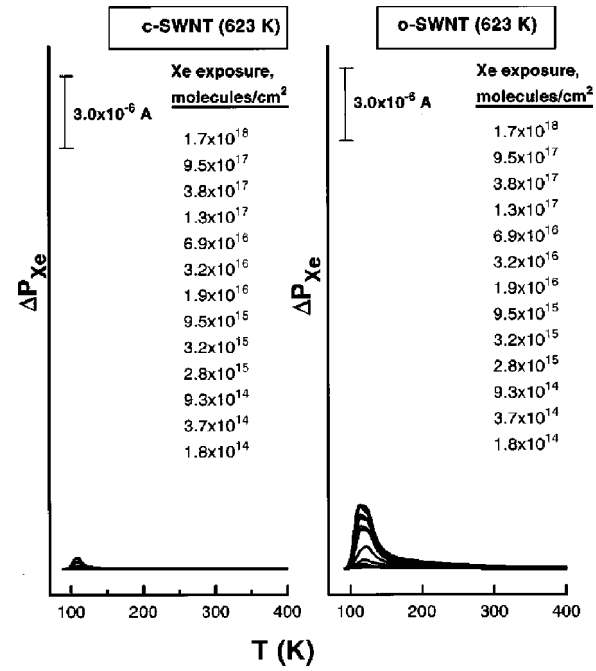

FIGURE 4. Temperature-programmed desorption (TPD) of Xe on closed (c-SWNTs) and chemically opened SWNTs (o-SWNTs). The area of the desorption traces is proportional to the Xe coverage achieved at a given exposure to Xe(g). The capacity is significantly increased by opening the c-SWNTs, as is the initial sticking coefficient (not shown). Reused with permission from A. Kuznetsova, Journal of Chemical Physics, 112, 9590 (2000). Copyright 2000, American Institute of Physics.

2. Molecular Access into the Nanotube Interior

In the synthesized material, nanotube ends are closed by hemispherical fullerene-like caps[14] that block molecular access into the nanotube interior. However, it is the nanotube interior that presents the most interest for the adsorption of molecules as far as potential practical applications are concerned, because of its deep potential well and significant capacity.[10,15]

Thus, an opening process is needed that is capable of removing the end caps. Kuznetsova[16] observed that an aqueous phase acidic oxidative process developed by the Smalley group[17] and usually employed for nanotube purification also opens the end caps for Xe adsorption. This purification procedure is used to dissolve graphitic impurities and Ni-Co catalyst particles present in the as-synthesized SWNTs. The procedure consists of treatment with an aqueous solution of HNO_3/H_2SO_4 followed by sonication in aqueous H_2O_2/H_2SO_4.[17] Aside from opening the end caps, this procedure also results in the cutting of the SWNTs, decreasing the average length of the nanotubes in the sample. It was found that after purification (followed by annealing in vacuum at 623 K to eliminate the oxygen-containing functional groups) both the capacity and the sticking coefficient of SWNTs toward Xe at 95 K were greatly enhanced. This effect can be seen in the temperature-programmed desorption (TPD) traces of Xe for purified and unpurified material in Figure 4. The area under the TPD trace is directly proportional to the amount

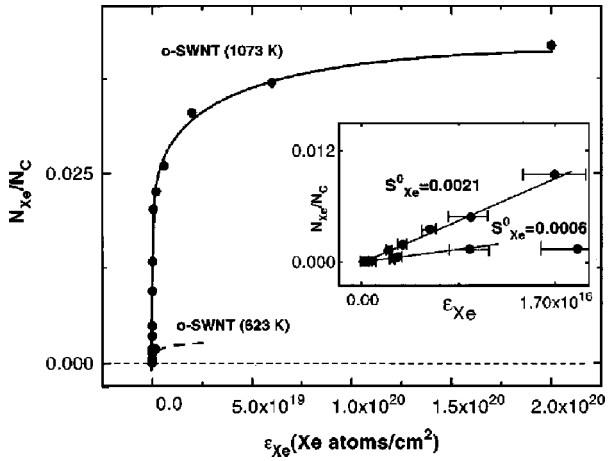

FIGURE 5. Removing the functional groups from oxidatively etched SWNTs increases the adsorptive capacity by a factor of ~20. The sticking coefficient (inset) is increased by a factor of approximately 3.5. Reused with permission from A. Kuznetsova, Journal of Chemical Physics, 112, 9590 (2000). Copyright 2000, American Institute of Physics.

of Xe adsorbed on the SWNTs. After the oxidative treatment, the adsorption capacity of the SWNTs increased by a factor of 12, while the sticking coefficient (the probability that an incoming gas phase Xe atom will be adsorbed on the surface) increased by a factor of 6.

Furthermore, it was found that heating the chemically etched material to a high temperature (1073 K) increases the capacity and the sticking coefficient even further.[16,18] Such heating is accompanied by the evolution of CH_4, CO, H_2, and CO_2 gases from the SWNT sample. This implies that there are functional groups on unannealed oxidized SWNTs that somehow block the entry ports created by the oxidative chemical etching. Removing these functional groups through annealing maximizes the adsorptive capacity of SWNTs (Figure 5), leading to a further increase in the adsorption capacity by a factor of ~20.

Evidence for the disappearance of specific functional groups from the SWNTs after heating in vacuum has been obtained by transmission IR spectroscopy. Carbonyl groups and C–O single bonds, as well as OH groups, were detected by IR spectroscopy on oxidized SWNTs before heating.[18] As the temperature is gradually increased, these groups are destroyed (Figure 6). The presence and decomposition of these groups during heating to 1073 K were also verified with near-edge X-ray absorption fine structure spectroscopy (NEXAFS).[19] This study enabled the determination of the oxygen-to-carbon ratio, O/C, which was measured to be 5.5–6.7% on the oxidized SWNTs. On the other hand, nanotubes that had not been treated with oxidizing acidic solutions had an O/C ratio of only 1.9%. It was found that the most stable groups containing oxygen involve C–O single bonds. Raman spectral measurements indicated that the carbon bond structure of the nanotubes themselves was not perturbed by the heating, as expected for a highly stable sp^2-hybridized conjugated configuration.

A similar fraction of carbon atoms at defects, ~5%, was found for chemically etched nanotubes in a study where the

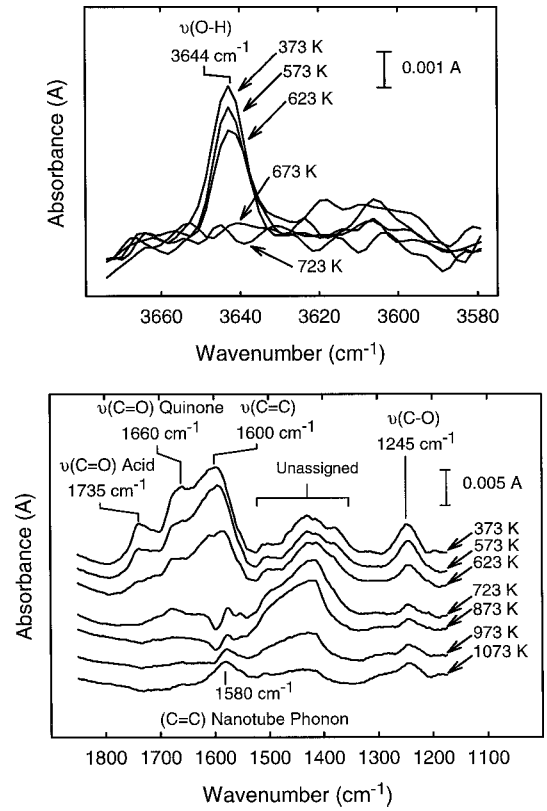

FIGURE 6. Decomposition of the functional groups introduced onto SWNTs by the oxidizing chemical etching, as observed by transmission IR spectroscopy in vacuum. Carbonyl and ester groups present on SWNTs decompose as the annealing temperature is increased. Reprinted with permission from A. Kuznetsova, Chemical Physics Letters 321, 292 (2000). Copyright 2000, Elsevier.

defect density in the SWNT walls was determined experimentally by titration with a reactive oxidizing molecule, ozone.[20,21] Ozone readily reacts with carbon atoms at the vacancy defect sites, as well as carbon atoms at the nanotube ends. The reaction with a defect-free nanotube surface should, however, be far slower. By exposing nanotubes to ozone, then heating them to a high temperature (1273 K) to remove the oxygen-containing functional groups, and measuring the amount of carbon in the evolved CO_2 and CO, one can estimate the fraction of carbon atoms located at defect sites. The experiment indicated that $5 \pm 2.5\%$ of the carbon atoms are located at defects. This defect density is far greater than the fraction of carbon atoms on the perimeter of the open ends of the nanotubes,[20] indicating that reactions with defect sites in the SWNT walls will dominate the etching process either in an oxidizing acidic etching solution or in O_3.

Ozone treatment and subsequent annealing to liberate CO and CO_2 were also found to enhance the adsorptive capacity of the SWNTs for Xe. If many successive cycles of treatment with O_3 and annealing to 973 K are carried out, the adsorptive capacity initially increases and then decreases.[22] The increase is explained by ozone expanding the diameter of entry ports already present on the walls of the nanotubes, as well as introducing new ones. After a certain point, however, the loss of carbon through CO and CO_2 formation leads to a reduction in the adsorptive

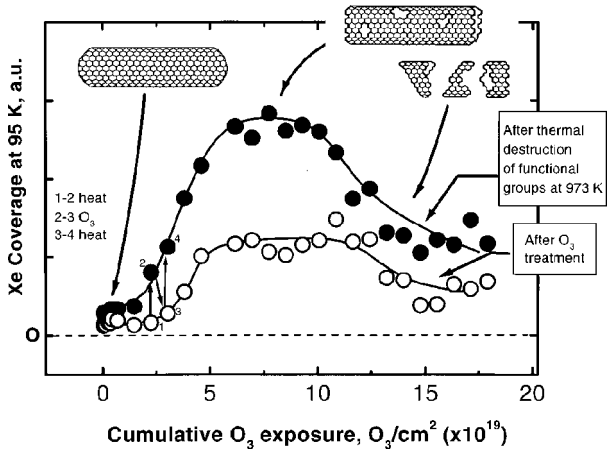

FIGURE 7. Evolution of the Xe adsorption capacity of SWNTs with successive cycles of O_3 etching and annealing at 973 K. The top curve corresponds to adsorption capacity after annealing to remove blocking functional groups; the bottom curve is the adsorption capacity after treatment with O_3, but before annealing. Reused with permission from A. Kuznetsova, Journal of Chemical Physics, 115, 6691 (2001). Copyright 2001, American Institute of Physics.

capacity (Figure 7). Through the entire ozone-etching process it is seen that when the SWNT sample is functionalized with oxygen-containing groups, it exhibits a lower adsorption capacity, due to blocking of the entry ports by strongly dipolar oxygen-containing functionalities.

Other oxidation methods also cause the opening of the SWNTs. Jakubek and Simard[23] used oxidation in dry air at 475 K to open the nanotubes. As with our results, the surface area increased, and the microporous area approximately tripled after a 2 h oxidation treatment.

Mechanical ball milling with diamond particles has similarly been demonstrated to enhance molecular access into the SWNT interior.[24] After the ball-milling procedure, an additional step appears in the adsorption isotherms of CCl_4 on SWNTs at low partial pressures. The authors attribute this isotherm feature to the interior-bound CCl_4.

Experiments of Matranga and Bockrath,[25] as well as those of Lafi et al.,[1] emphasize the importance of removing the functional groups from the entry ports into the nanotubes for molecular adsorption. Interestingly, Matranga reports that the controlled introduction of such blocking groups can also be used to lock small quantities of gases (SF_6 and CO_2) in SWNTs. After the functional groups are removed by heating, the gases can be adsorbed in the SWNTs at cryogenic temperatures. If the SWNTs with the molecules adsorbed inside are then treated with ozone, the adsorbed molecules will be prevented from exiting by the added functional groups. The authors report that samples of SWNTs with SF_6 or CO_2 blocked inside are stable in vacuum over periods of 24 h and can withstand exposure to air.

3. Resolution of SWNT Adsorption Sites by Temperature-Programmed Desorption and IR Spectroscopy

Different types of well-defined adsorption sites in SWNTs place the adsorbed molecules in different environments. This allows distinguishing between the various sites by using adsorbed molecules as probes for their environment. The most straightforward and easily detectable difference is the adsorption energy. Temperature-programmed desorption (TPD) can be successfully employed for this purpose, as it exploits differences in the desorption activation energies, which control the desorption kinetics. Figure 8 shows experimentally obtained TPD spectra of *n*-pentane on opened SWNTs, compared to the Monte Carlo (MC) simulation of the desorption process.[13] TPD spectra obtained in a rapidly pumped ultrahigh vacuum system correspond closely to the derivatives of the coverage present with respect to time at a given temperature during the programmed heating process.[26]

Four resolved spectral peaks are visible in the TPD spectra of pentane. It has to be noted that such resolution of desorption peaks, while not unusual on single crystalline surfaces, is rarely seen for high-area materials. By comparison of the experimentally observed peaks to the MC simulation of desorption from nanotube interior, groove and exterior sites, where the coverage is plotted versus the temperature, the highest desorption temperature peak can be assigned to the interior sites, the next highest to the groove sites on the outside of SWNT bundles, and the next highest to the nanotube exterior surface. The sharply peaked low-temperature feature in the experimental TPD spectra corresponds to multilayer desorption and is not characteristic of the nanotube adsorption sites.

This same progression of adsorption sites as seen here for *n*-pentane can be observed for a range of molecules. For instance, all normal alkanes demonstrate virtually identical spectra, differing only in the fact that the desorption temperatures for the three types of sites increase for longer alkane molecules that exhibit increasing polarizabilities. This comparison is seen for five alkanes in Figure 9.

A tetrahedral molecule, CCl_4, also occupies the same sites on SWNTs and displays four similar features in the TPD spectra. If it is coadsorbed on SWNTs with normal nonane for example, the two molecules will compete for adsorption sites. The result for the coadsorption of CCl_4 and *n*-nonane is depicted in Figure 10. Initially, CCl_4 populates only the interior sites. As *n*-nonane molecules are more polarizable and consequently have a higher adsorption energy, adding *n*-nonane when CCl_4 is adsorbed on the interior SWNT sites will result in the displacement of CCl_4 into adsorption sites with lower adsorption energies, i.e., first into groove sites and then onto the exterior and into the multilayer.[27]

The vibrational frequencies of a molecule in infrared or Raman spectroscopy can also provide information about the environment of the adsorbed molecule. Generally, the more strongly the adsorbed molecule interacts with the surface through dispersive forces, the more redshifted the frequencies of its vibrational modes become relative to an isolated molecule. This phenomenon can be viewed as the dispersive forces flattening somewhat

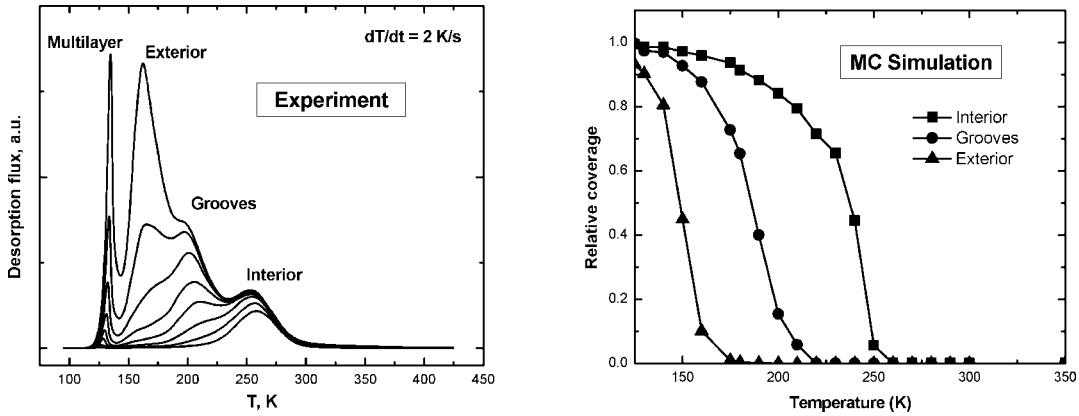

FIGURE 8. TPD spectra of *n*-pentane for increasing exposures (left) and an MC simulation of the desorption process from three types of adsorption sites (right). The derivatives of the data from the simulation correspond approximately to the peaks in the experimental spectra on the left. On the basis of the comparison between the simulation and experiment, the assignment of the TPD peaks can be made. Right panel reprinted with permission from ref 13. Copyright 2005 American Chemical Society.

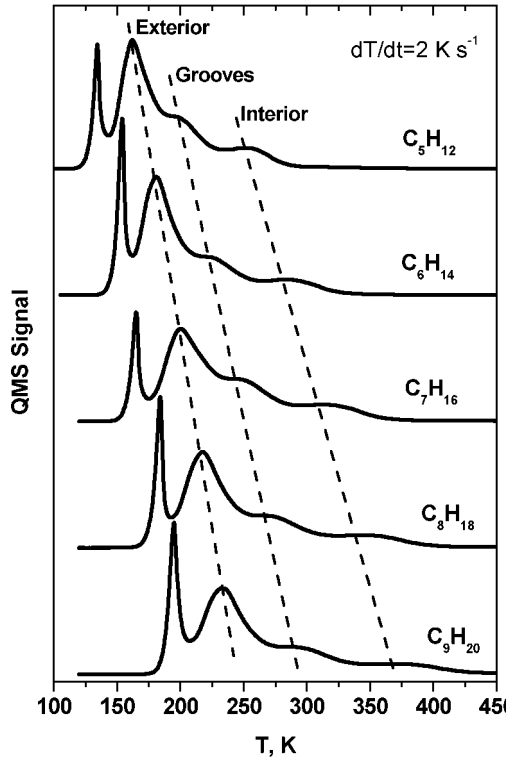

FIGURE 9. Comparison of temperature-programmed desorption traces for five normal alkanes, pentane to nonane, from SWNTs. The same four peaks are present for all molecules, and an increase in the desorption temperature for each adsorption site is seen as the number of carbon atoms in the chain increases.[13]

the potential well of the vibrational motion, leading to a lower frequency.

It has been found that the asymmetric stretch mode of interior-adsorbed CF_4 (at 1247 cm^{-1}) is red-shifted relative to the gas phase CF_4 molecule (1282 cm^{-1}). It is also red-shifted with respect to the same mode in the exterior-adsorbed species (1267 cm^{-1}),[28] as shown in the schematic in Figure 11. This implies that the molecule interacts more strongly with the nanotube walls when it is adsorbed in the interior. Significant infrared absorption associated with the CF_4 adsorbed in the nanotube interior sites appeared only after the nanotubes were opened by treatment with gaseous O_3 followed by annealing to 873 K, building on earlier work where such treatment was seen to increase both the rate of adsorption and adsorption capacity for Xe.[22]

Qualitatively similar red shifts were seen in the case of adsorption of NO on SWNTs.[29] Upon NO adsorption, the molecules dimerized, forming $(NO)_2$, with the asymmetric stretch vibration for the interior-adsorbed dimer occurring at 1257 cm^{-1}, while the gas phase frequency for this vibration is known to be 1289 cm^{-1}.

The C–C vibrations in ethane and propane and the symmetric stretch in SF_6 were also seen to produce red-shifted features in Raman spectra following adsorption on multiwall carbon nanotubes.[30]

4. Molecular Packing in the Interior and Groove Sites

The ability to observe molecules in different adsorption sites by TPD opens possibilities of exploring molecular behavior in those sites. As the spatial configurations of the groove sites and interior sites differ significantly, measuring adsorption capacities of the nanotube interior and grooves for molecules of different shapes should provide insight into the packing of molecules in these sites. Capacities can be measured in a relatively straightforward way from TPD data by integrating the areas under the TPD peaks corresponding to each adsorption site.

Using this technique for linear and branched alkanes, we have shown that the number of molecules that can fit in groove sites at maximum coverage depends on the length of the adsorbed molecule, while the number of molecules that can fit in interior nanotube sites (at maximum coverage) depends on the molecular volume.[13]

This result is due to the fact that the narrow groove sites closely approximate a one-dimensional adsorption site, while the nanotube interior has a sizable accessible diameter [approximately 10 Å for a (10,10) nanotube] compared to typical diameters of molecules that can be adsorbed from the gas phase. In MC simulations of Xe

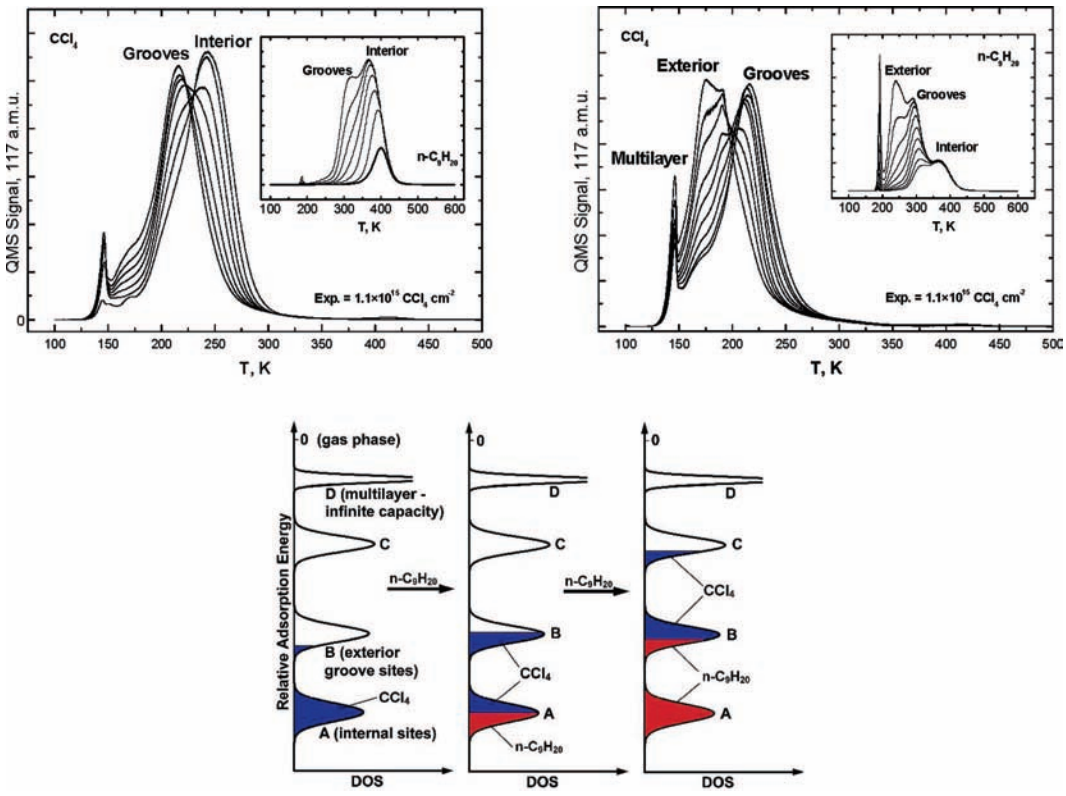

FIGURE 10. TPD spectra (top) for co-adsorbed CCl_4 and *n*-nonane (insets). The amount of CCl_4 remains constant. As the amount of *n*-nonane is increased from zero coverage, the CCl_4 is first displaced into the groove sites (left) and then onto the nanotube exterior and into the multilayer (right). Density-of-states diagram (bottom) illustrating the displacement process. Reprinted with permission from P. Kondratyuk, Chemical Physics Letters 410, 324 (2005). Copyright 2005, Elsevier.

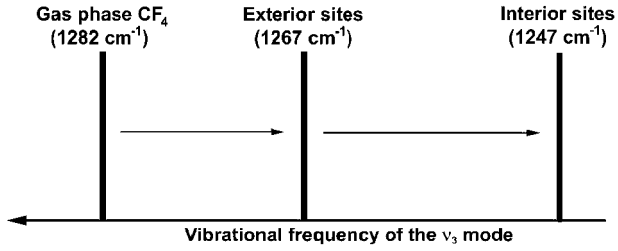

FIGURE 11. Shift to a lower frequency of the ν_3 vibrational mode of CF_4 following adsorption on SWNTs, as seen by transmission FTIR spectroscopy. The red shift for the interior-adsorbed CF_4 is significantly larger compared to the exterior-adsorbed CF_4.[28]

adsorption in SWNTs,[22] it was seen that the Xe atoms fill all the available space inside nanotubes in a closely packed manner.

Figure 12 compares the relative amounts of space occupied in the groove sites by five linear alkanes, pentane to nonane, and a branched octane molecule, 2,2,4-trimethylpentane. The amount of space occupied in a site is a quantity inversely proportional to the capacity of the site for that molecule. It was seen that the branched octane molecule occupies far less space in the groove than a linear octane molecule, even though their molar volumes in the bulk are essentially the same. In fact, the branched octane molecule occupies approximately as much space in the groove as a hexane molecule. These experimental results matched well the results of MC simulations of alkane adsorption in SWNT grooves.[13] This shows that for groove sites, the length of the molecule determines the packing density, with longer molecules occupying more space.

In contrast, simulations show that in the nanotube *interior* the branched octane takes up almost exactly the same amount of space as the linear octane (Figure 13). This means that for the interior, where molecules are relatively unconstrained by adsorption site geometry, the packing density is determined by the molecular volume rather then length.

5. Shielding of Interior-Adsorbed Molecules by SWNTs

Shielding of molecular species adsorbed on porous material from chemical reactants arriving from the outside is an expected effect. After all, the attacking molecule needs to find a way to the adsorbate in the high-area material, and steric shielding by the solid should lead to a decrease in reaction rate. However, nanotubes with their regular tubular geometry offer the unique ability to hide a molecule in their interior, and our TPD method of analysis enables one to look for the shielding when nanotubes serve as molecular scale containers, that is, to observe a decrease in reaction rate with incident species when the reactant molecules are adsorbed *inside* carbon nanotubes. There is a significant new kinetic hurdle for the incoming molecule: finding the point of entry into the nanotube, entering the nanotube, and diffusing inside the nanotube to react with the adsorbate.

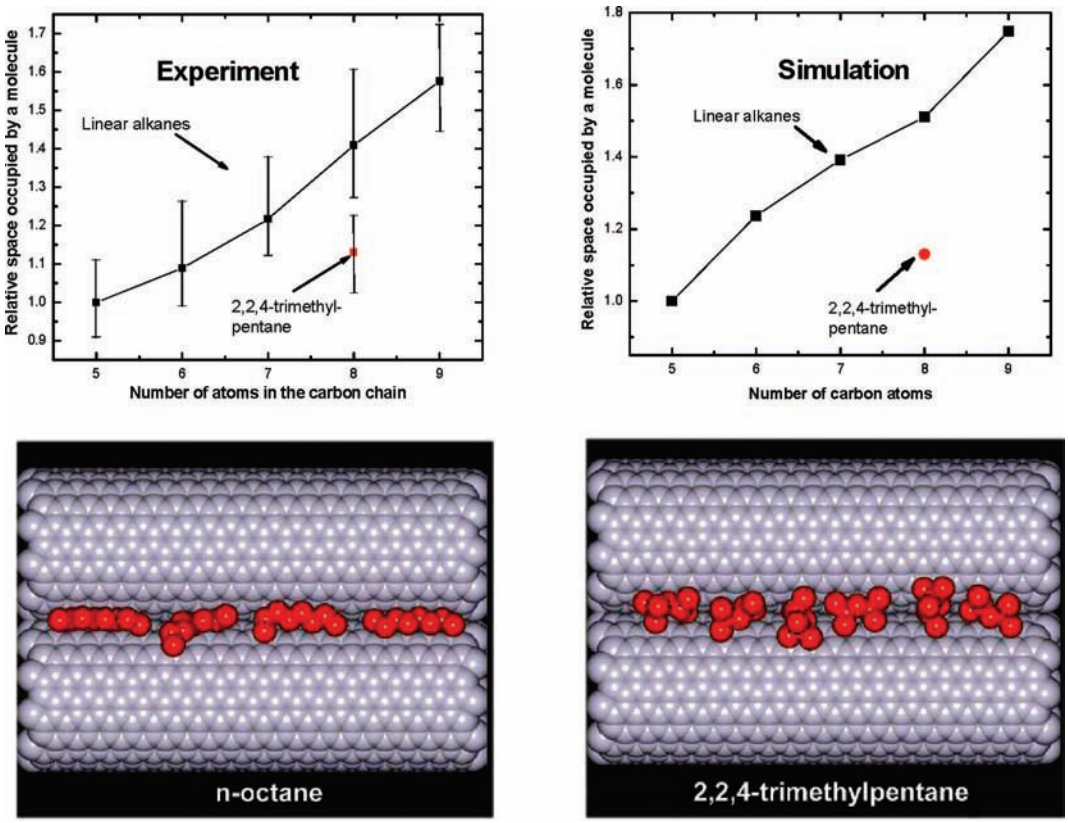

FIGURE 12. Top: Amount of space occupied in the groove sites by five linear alkanes and a branched octane, 2,2,4-trimethylpentane, from experiments and MC simulations. The branched octane molecule occupies approximately as much space as linear hexane, demonstrating that the capacity of groove sites depends on the molecular length. Bottom: Snapshots from the simulations of the linear and branched octane molecules in the groove sites. Reprinted with permission from ref 13. Copyright 2005, American Chemical Society.

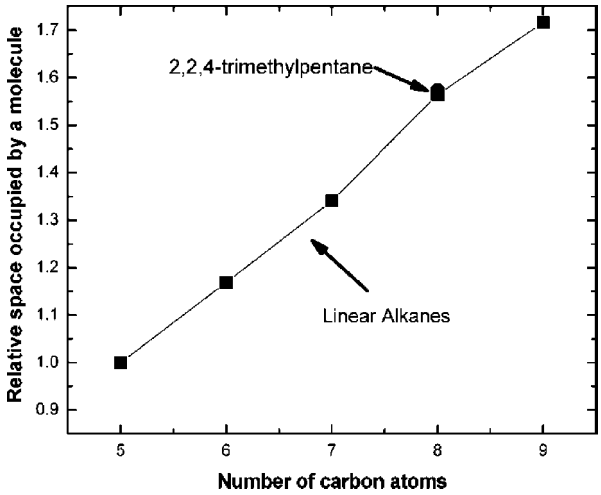

FIGURE 13. Amount of space occupied in the interior sites of SWNTs for linear alkanes and a branched octane from MC simulations. A branched octane molecule occupies as much space as a linear octane, meaning that the capacity of the internal sites is determined by the molecular volume, not length. Reprinted with permission from ref 13. Copyright 2005, American Chemical Society.

As a model reaction, we chose the hydrogenation of 1-heptene by atomic hydrogen. This reaction proceeds in the condensed phase even at cryogenic temperatures, first producing secondary alkyl radicals, which then undergo disproportionation to produce fully reduced alkane.[32] Thus, the reactivity can be determined by monitoring the rate of production of *n*-heptane at a given flux of atomic hydrogen radicals. To discount the macroscopic shielding effect of porous materials on reactivity mentioned above, a comparison of reactivity was made for nanotube interior sites and groove sites, where any effect of the porosity of the SWNT sample would be offset. We found that the reactivity for *n*-heptene species in the interior was significantly lower than for *n*-heptene in the groove sites, as shown in Figure 14, which depicts the fraction of hydrogenated 1-heptene versus the exposure to atomic hydrogen. The two curves correspond to 1-heptene being present in the interior sites only (bottom curve) and simultaneously in the interior and groove sites (top curve). For similar exposures to atomic H, the converted fraction is on average ~3.2 times higher when 1-heptene is present in the groove sites, meaning that groove sites are more readily accessible by the atomic H than the interior sites. The reactivity of a multilayer of 1-heptene adsorbed on a flat gold surface without SWNTs is shown as a single point for comparison.[31]

6. Changes in the Adsorbates Due to Confinement in SWNTs

Spatial confinement of molecules by their adsorption in SWNTs results in significant changes in their properties compared to those of the bulk phase. A number of examples have been described by our group as well as by

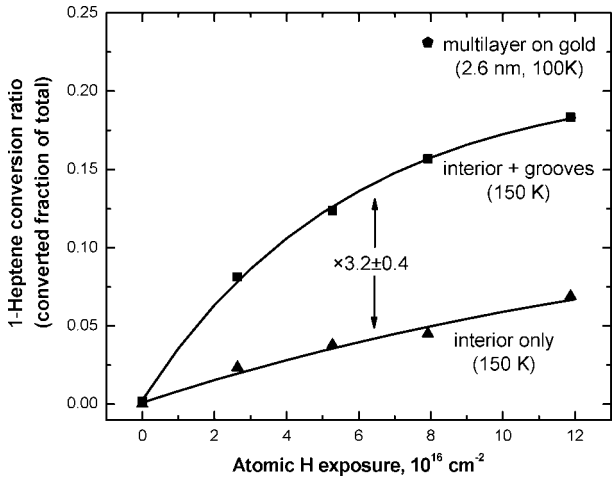

FIGURE 14. Fraction of hydrogenated 1-heptene vs exposure to atomic H, for 1-heptene adsorbed exclusively in the interior sites, and simultaneously in the interior and groove sites. Reactivity in the case when 1-heptene is present in the groove sites is significantly higher. The single point for the reactivity of a 1-heptene multilayer on gold is given for comparison. Reprinted with permission from ref 31. Copyright 2007, American Chemical Society.

other authors that suggest a possible use of nanotubes as atomic-scale templates for producing specific arrangements of matter having special properties.

It has been proposed that adsorption in carbon nanotubes can produce a system in which the adsorbate will behave as one-dimensional fluid, both from the classical and quantum mechanical points of view.[10,33] Evidence for such one-dimensional behavior was seen experimentally in the adsorption isotherms of Xe and Ar on SWNT bundles[33] and in the heat capacity of ^{4}He adsorbed on SWNTs at 100 mK and 6 K.[34]

Theoretical calculations predicting that He atoms or H_2 molecules will undergo Bose–Einstein condensation when adsorbed in the interstitial channels present in bundles of SWNTs have been reported.[35]

When water molecules are confined inside of nanotubes at cryogenic temperatures, a new hydrogen-bonded structure results that has a characteristic infrared signature.[36] MC simulations show that water molecules inside SWNTs form a layered cylindrical structure (Figure 15).

In the case of a (10,10) nanotube, each layer is composed of seven water molecules hydrogen-bonded into a heptagonal ring. Narrower nanotubes produce water rings with a smaller number of water molecules. The hydrogen atoms not taking part in the intra-ring bonding form hydrogen bonds with neighboring rings, as demonstrated in Figure 15B. Such layered structures are stable at temperatures up to 270 K in (10,10) nanotubes, while for more narrow nanotubes, the range of temperature stability extends even higher.

MD simulations of water in SWNTs were performed to calculate the vibrational frequencies of O–H bonds due to intra-ring and inter-ring hydrogens. The simulations indicate that the intra-ring hydrogen bonds are bulk-like, while the inter-ring bonds have a distorted geometry and are weakened as a result. The hydrogen

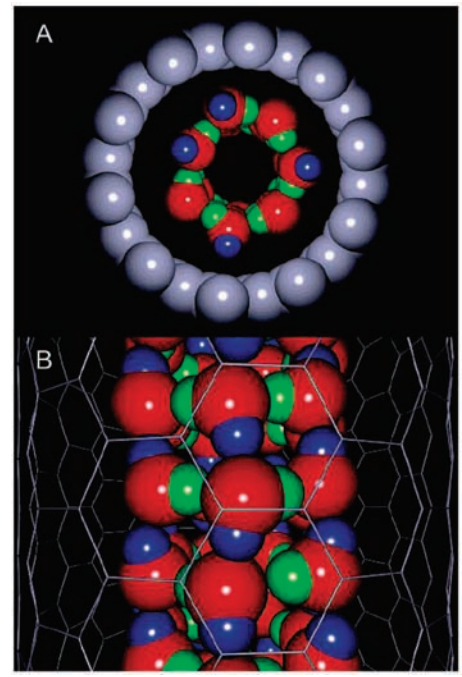

FIGURE 15. Structure of water inside (10,10) SWNTs at 123 K seen in a MC simulation [end view (A) and side view (B)]. Water molecules form heptagonal rings. Oxygen atoms are shown as red spheres, hydrogens that form inter-ring hydrogen bonds as blue spheres, and those forming intra-ring bonds as green spheres. The mesh structure in panel B represents carbon–carbon bonds of the SWNT. Reprinted with permission from ref 36. Copyright 2006, American Chemical Society.

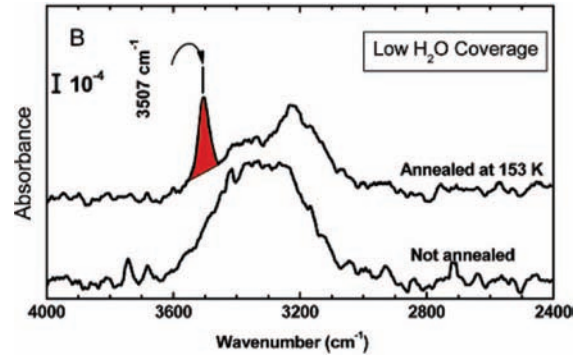

FIGURE 16. Appearance of the vibrational mode due to water molecules confined in SWNTs in an ordered ring structure. As the SWNTs with water deposited at 123 K are annealed, water molecules migrate into interior sites of SWNTs, producing the 3507 cm^{-1} O–H stretching mode. Reprinted with permission from ref 36. Copyright 2006, American Chemical Society.

atoms taking part in such weak bonds give rise to a distinct sharp O–H stretching mode. This vibrational mode stands out from other O–H stretching vibrations that result in a broad peak in experimental IR spectra, as shown in Figure 16. After the water molecules have been deposited on the SWNT surface at 123 K, annealing at 153 K allows the water molecules to diffuse into the SWNTs, leading to the appearance of the mode associated with the inter-ring hydrogen bonds at 3507 cm^{-1}. The interior adsorption of H_2O may be effectively blocked using *n*-nonane.[36,37]

7. Enhancement of Molecular Transport inside SWNTs

With a view to an area of application in nanoporous membranes, a number of workers studied diffusion and molecular transport in nanotubes, both experimentally[38,39] and theoretically.[40,41]

Theoretical studies show that diffusion inside nanotubes should be rapid at low concentrations of molecules, mainly due to the smoothness of the potential along the nanotube wall, meaning that the diffusing molecule undergoes few scattering events. As the concentration increases, the molecules begin to scatter on each other and the diffusion coefficient decreases.[41] However, there are strong indications that even at high adsorbate densities the diffusion of molecules inside SWNTs is significantly faster than in the bulk. It was recently found that even at full loading the self-diffusion coefficient of *n*-heptane in SWNTs is larger by a factor of 35 than the self-diffusion coefficient in bulk *n*-heptane at the same temperature.[42] This is the result of molecular ordering of the confined adsorbate in the nanotubes. *n*-Heptane molecules tend to orient themselves parallel to the nanotube axis when they are adsorbed inside SWNTs. This makes translational motion along the nanotube axis less hindered, thus increasing the diffusion coefficient. A similar increase in diffusivity due to the formation of ordered structure is seen in the simulations of N_2 diffusion in SWNTs,[40] where an ordered row of molecules is formed in the nanotube center.

When the motion of molecules is concerted rather than random, the smoothness of the potential along the nanotube walls provides a dramatic enhancement of transport properties over those predicted by hydrodynamic flow equations. Majumder et al.[38] measured the flow rates through a membrane composed of aligned multiwall carbon nanotubes for several liquids (water, alkanes, and alcohols). The flow rates were found to be 4–5 orders of magnitude more rapid than the rates predicted by the hydrodynamic equations. Additionally, the flow rate did not correlate with the viscosity of the liquid. The authors attribute both of these effects to a nearly frictionless nanotube–liquid interface.

8. Summary and Future Expectations

Nanotubes provide a large specific surface area and a strong van der Waals binding energy for molecular adsorbates on well-defined adsorption sites. The interior sites have been shown experimentally and theoretically to exhibit the highest binding energy, followed by the groove sites on the outside of SNWT bundles and the exterior sites on the convex outer surface, which have the lowest binding energy. The interstitial sites appear to be inaccessible to the adsorbate molecules.

A chemical oxidation step is needed to produce entry ports into the nanotube interior at the tube ends and at wall defect sites. The chemical groups that form during the chemical oxidation at the rims of the entry ports need to be removed by annealing to ~1000 K as they prevent molecules from entering the nanotubes. Ball milling with diamond particles can also be employed for the opening of SWNTs.

Linear groove sites behave as one-dimensional adsorption space for the adsorbate molecules. The confinement of molecules such as water or hydrocarbons in the interior of nanotubes produces adsorbed phases that differ strongly from the bulk in their structure, reactivity, and transport properties.

If one were to venture a guess about the future research directions in the field, several possibilities come to mind. First, the role of defects will probably be under increased scrutiny with a view to the control that they can afford over SWNT electronic and chemical properties. It is already fairly clear that the oxidation needed for the opening of the nanotubes occurs at strained end caps and wall defects. It has lately been found that the response of SWNT electronic properties to donor and acceptor molecules is much stronger if the nanotubes have a large number of structural defects.[43] Secondly, the experimental work on nanotube membranes[38,39] is likely to develop into a broader field, owing to the transport properties of the nanotubes that are superior to those of zeolite pores, polymeric pores, and other porous materials.

The work we have described chronicles some of the discoveries made in the past several years on the adsorption of molecules inside and outside of carbon nanotubes. Using methods from spectroscopy, surface science, and theoretical analysis, it would seem that we are witnessing the opening of a fascinating and significant new area of surface chemistry. The physical adsorption of interesting molecules on nanotube bundles promises many more surprises as we sharpen our observational and modeling methods. We dedicate this review to the late Professor Richard E. Smalley, who first suggested to us that the surface properties of carbon single-walled nanotubes should be a rich field for surface chemists.

References

(1) Lafi, L.; Cossement, D.; Chahine, R. Raman spectroscopy and nitrogen vapour adsorption for the study of structural changes during purification of single-wall carbon nanotubes. *Carbon* **2005**, *43*, 1347–1357.

(2) Iijima, S. Helical microtubules of graphitic carbon. *Nature* **1991**, *354*, 56–58.

(3) Iijima, S.; Ichihashi, T. Single-Shell Carbon Nanotubes of 1-nm Diameter. *Nature* **1993**, *363*, 603–605.

(4) Bethune, D. S.; Kiang, C. H.; Devries, M. S.; Gorman, G.; Savoy, R.; Vazquez, J.; Beyers, R. Cobalt-Catalyzed Growth of Carbon Nanotubes with Single-Atomic-Layerwalls. *Nature* **1993**, *363*, 605–607.

(5) Kukovecz, A. Konya, Z. Kiricsi, I. Single Wall Carbon Nanotubes. In *Encyclopedia of Nanoscience and Nanotechnology*; Nalwa, H. S., Ed.; American Scientific Publishers, **2004**; Vol *9*, pp 923–946.

(6) Stan, G.; Bojan, M. J.; Curtarolo, S.; Gatica, S. M.; Cole, M. W. Uptake of gases in bundles of carbon nanotubes. *Phys. Rev. B* **2000**, *62*, 2173–2180.

(7) Pearce, J. V.; Adams, M. A.; Vilches, O. E.; Johnson, M. R.; Glyde, H. R. One-dimensional and two-dimensional quantum systems on carbon nanotube bundles. *Phys. Rev. Lett.* **2005**, *95*, 185302.

(8) Talapatra, S.; Zambano, A. Z.; Weber, S. E.; Migone, A. D. Gases do not adsorb on the interstitial channels of closed-ended single-walled carbon nanotube bundles. *Phys. Rev. Lett.* **2000**, *85*, 138–141.

(9) Rols, S.; Johnson, M. R.; Zeppenfeld, P.; Bienfait, M.; Vilches, O. E.; Schneble, J. Argon adsorption in open-ended single-wall carbon nanotubes. *Phys. Rev. B* **2005**, *71*, 155411.
(10) Stan, G.; Cole, M. W. Low coverage adsorption in cylindrical pores. *Surf. Sci.* **1998**, *395*, 280–291.
(11) Simonyan, V. V.; Johnson, J. K.; Kuznetsova, A.; Yates, J. T., Jr. Molecular simulation of xenon adsorption on single-walled carbon nanotubes. *J. Chem. Phys.* **2001**, *114*, 4180–4185.
(12) Rawat, D. S.; Heroux, L.; Krungleviciute, V.; Migone, A. D. Adsorption of xenon on purified HiPco single walled carbon nanotubes. *Langmuir* **2006**, *22*, 234–238.
(13) Kondratyuk, P.; Wang, Y.; Johnson, J. K.; Yates, J. T., Jr. Observation of a one-dimensional adsorption site on carbon nanotubes: Adsorption of alkanes of different molecular lengths. *J. Phys. Chem. B* **2005**, *109*, 20999–21005.
(14) Dresselhaus, M. S.; Dresselhaus, G.; Eklund, P. C. *Science of fullerenes and carbon nanotubes*; Academic Press: San Diego, 1996.
(15) Peigney, A.; Laurent, C.; Flahaut, E.; Bacsa, R. R.; Rousset, A. Specific surface area of carbon nanotubes and bundles of carbon nanotubes. *Carbon* **2001**, *39*, 507–514.
(16) Kuznetsova, A.; Yates, J. T., Jr.; Liu, J.; Smalley, R. E. Physical adsorption of xenon in open single walled carbon nanotubes: Observation of a quasi-one-dimensional confined Xe phase. *J. Chem. Phys.* **2000**, *112*, 9590–9598.
(17) Rinzler, A. G.; Liu, J.; Dai, H.; Nikolaev, P.; Huffman, C. B.; Rodriguez-Macias, F. J.; Boul, P. J.; Lu, A. H.; Heymann, D.; Colbert, D. T.; Lee, R. S.; Fischer, J. E.; Rao, A. M.; Eklund, P. C.; Smalley, R. E. Large-scale purification of single-wall carbon nanotubes: Process, product, and characterization. *Appl. Phys. A: Mater. Sci. Process.* **1998**, *67*, 29–37.
(18) Kuznetsova, A.; Mawhinney, D. B.; Naumenko, V.; Yates, J. T., Jr.; Liu, J.; Smalley, R. E. Enhancement of adsorption inside of single-walled nanotubes: Opening the entry ports. *Chem. Phys. Lett.* **2000**, *321*, 292–296.
(19) Kuznetsova, A.; Popova, I.; Yates, J. T., Jr.; Bronikowski, M. J.; Huffman, C. B.; Liu, J.; Smalley, R. E.; Hwu, H. H.; Chen, J. G. G. Oxygen-containing functional groups on single-wall carbon nanotubes: NEXAFS and vibrational spectroscopic studies. *J. Am. Chem. Soc.* **2001**, *123*, 10699–10704.
(20) Mawhinney, D. B.; Naumenko, V.; Kuznetsova, A.; Yates, J. T., Jr.; Liu, J.; Smalley, R. E. Surface defect site density on single walled carbon nanotubes by titration. *Chem. Phys. Lett.* **2000**, *324*, 213–216.
(21) Mawhinney, D. B.; Naumenko, V.; Kuznetsova, A.; Yates, J. T., Jr.; Liu, J.; Smalley, R. E. Infrared spectral evidence for the etching of carbon nanotubes: Ozone oxidation at 298 K. *J. Am. Chem. Soc.* **2000**, *122*, 2383–2384.
(22) Kuznetsova, A.; Yates, J. T., Jr.; Simonyan, V. V.; Johnson, J. K.; Huffman, C. B.; Smalley, R. E. Optimization of Xe adsorption kinetics in single walled carbon nanotubes. *J. Chem. Phys.* **2001**, *115*, 6691–6698.
(23) Jakubek, Z. J.; Simard, B. Two confined phases of argon adsorbed inside open single walled carbon nanotubes. *Langmuir* **2004**, *20*, 5940–5945.
(24) Babaa, M. R.; Dupont-Pavlovsky, N.; McRae, E.; Masenelli-Varlot, K. Physical adsorption of carbon tetrachloride on as-produced and on mechanically opened single walled carbon nanotubes. *Carbon* **2004**, *42*, 1549–1554.
(25) Matranga, C.; Bockrath, B. Controlled confinement and release of gases in single-walled carbon nanotube bundles. *J. Phys. Chem. B* **2005**, *109*, 9209–9215.
(26) Yates, J. T., Jr. The thermal desorption of adsorbed species. *Methods Exp. Phys.* **1985**, *22*, 425–464.
(27) Kondratyuk, P.; Yates, J. T., Jr. Desorption kinetic detection of different adsorption sites on opened carbon single walled nanotubes: The adsorption of n-nonane and CCl_4. *Chem. Phys. Lett.* **2005**, *410*, 324–329.
(28) Byl, O.; Kondratyuk, P.; Forth, S. T.; FitzGerald, S. A.; Chen, L.; Johnson, J. K.; Yates, J. T., Jr. Adsorption of CF_4 on the internal and external surfaces of opened single-walled carbon nanotubes: A vibrational spectroscopy study. *J. Am. Chem. Soc.* **2003**, *125*, 5889–5896.
(29) Byl, O.; Kondratyuk, P.; Yates, J. T., Jr. Adsorption and dimerization of NO inside single-walled carbon nanotubes: An infrared spectroscopic study. *J. Phys. Chem. B* **2003**, *107*, 4277–4279.
(30) Matranga, C.; Bockrath, B.; Chopra, N.; Hinds, B. J.; Andrews, R. Raman spectroscopic investigation of gas interactions with an aligned multiwalled carbon nanotube membrane. *Langmuir* **2006**, *22*, 1235–1240.
(31) Kondratyuk, P.; Yates, J. T., Jr. Effects of Molecular Confinement inside Single Walled Carbon Nanotubes on Chemical Reactivity: Atomic H + 1-heptene. *J. Am. Chem. Soc.* **2007**, submitted for publication.
(32) Klein, R.; Scheer, M. D.; Kelley, R. Disproportionation-combination reactions of alkyl radicals and hydrogen atoms at low temperatures. *J. Phys. Chem.* **1964**, *68*, 598–605.
(33) Talapatra, S.; Migone, A. D. Existence of novel quasi-one-dimensional phases of atoms adsorbed on the exterior surface of close-ended single wall nanotube bundles. *Phys. Rev. Lett.* **2001**, *8720*, 206106.
(34) Lasjaunias, J. C.; Biljakovic, K.; Sauvajol, J. L.; Monceau, P. Evidence of 1D behavior of He-4 confined within carbon-nanotube bundles. *Phys. Rev. Lett.* **2003**, *91*, 025901.
(35) Ancilotto, F.; Calbi, M. M.; Gatica, S. M.; Cole, M. W. Bose-Einstein condensation of helium and hydrogen inside bundles of carbon nanotubes. *Phys. Rev. B* **2004**, *70*, 165422.
(36) Byl, O.; Liu, J. C.; Wang, Y.; Yim, W. L.; Johnson, J. K.; Yates, J. T., Jr. Unusual hydrogen bonding in water-filled carbon nanotubes. *J. Am. Chem. Soc.* **2006**, *128*, 12090–12097.
(37) Byl, O.; Liu, J.; Yates, J. T., Jr. Characterization of single wall carbon nanotubes by nonane preadsorption. *Carbon* **2006**, *44*, 2039–2044.
(38) Majumder, M.; Chopra, N.; Andrews, R.; Hinds, B. J. Nanoscale hydrodynamics: Enhanced flow in carbon nanotubes. *Nature* **2005**, *438*, 44.
(39) Hinds, B. J.; Chopra, N.; Rantell, T.; Andrews, R.; Gavalas, V.; Bachas, L. G. Aligned multiwalled carbon nanotube membranes. *Science* **2004**, *303*, 62–65.
(40) Arora, G.; Wagner, N. J.; Sandler, S. I. Adsorption and diffusion of molecular nitrogen in single wall carbon nanotubes. *Langmuir* **2004**, *20*, 6268–6277.
(41) Jakobtorweihen, S.; Verbeek, M. G.; Lowe, C. P.; Keil, F. J.; Smit, B. Understanding the loading dependence of self-diffusion in carbon nanotubes. *Phys. Rev. Lett.* **2005**, *95*, 044501.
(42) Kondratyuk, P.; Wang, Y.; Liu, J.; Johnson, J. K.; Yates, J. T., Jr. Inter- and intratube self-diffusion in n-heptane adsorbed on carbon nanotubes. *J. Phys. Chem. C* **2007**, *111*, 4578–4584.
(43) Robinson, J. A.; Snow, E. S.; Badescu, S. C.; Reinecke, T. L.; Perkins, F. K. Role of defects in single-walled carbon nanotube chemical sensors. *Nano Lett.* **2006**, *6*, 1747–1751.

AR700013C